Translational Oncology
www.transonc.com

Volume 7 Number 2 pp. 213–220 213

Molecular Imaging of Oral Premalignant and Malignant Lesions Using Fluorescently Labeled Lectins

John Baeten*, Amritha Suresh†, Alexander Johnson*, Ketan Patel‡, Moni Kuriakose†, Anita Flynn† and Deepak Kademani‡

* Inter-Med Inc., Vista Dental Products, 2200 Northwestern Ave., Racine, WI 53404, USA; †Mazumdar-Shaw Cancer Center, Department of Head and Neck Oncology, Narayana Health City, 258/A, Bommasandra Industrial Area, Anekal Taluk 560 099, Bangalore, India; ‡University of Minnesota, Department of Oral and Maxillofacial Surgery, Moos Tower 7-174G, 515 Delaware Street, Minneapolis, MN 55455, USA

Abstract

Aberrant glycosylation during carcinogenesis results in altered glycan expression on oral cancer cells. The objective of this study was to detect this atypical glycosylation *via* imaging of fluorophore-conjugated lectins. Paired normal and tumor tissue from seven patients with oral squamous cell carcinoma were investigated for sialic acid expression *via* the legume protein wheat germ agglutinin (WGA). Fluorophore (Alexa Fluor 350 and Alexa Fluor 647) conjugated WGA was topically applied to the tissue samples and imaged using a custom wide-field fluorescence imaging system. All seven patients had histologically confirmed disease with 6/7 exhibiting squamous cell carcinoma and 1/7 exhibiting dysplasia. Fluorescent data collected from all patients demonstrated that fluorophore conjugated WGA could distinguish between pathologically normal and diseased tissue with the average signal-to-noise ratio (SNR) among all patients being 5.88 (P = .00046). This SNR was statistically significantly higher than the SNR from differences in tissue autofluorescence (P = .0049). A lectin inhibitory experiment confirmed that lectin binding is molecularly specific to overexpressed tumor glycans and that fluorescence is not due to tissue optical properties or tissue diffusion differences. These results illustrate that changes in tumor glycan content of oral neoplasms can be detected with optical imaging using topically applied fluorescently labeled WGA. Lectin targeting of oral lesions using optical imaging may provide a new avenue for the early detection of oral cancers.

Translational Oncology (2014) 7, 213–220

Introduction

Oral cancer, which includes cancers of the lips, tongue, cheeks, floor of the mouth, hard and soft palate, sinuses, and pharynx (throat), is the sixth most common cancer nationally and the third most prevalent cancer in developing countries [1–3]. Oral cancer's five year survival rate has slightly increased over the past four decades to 65% in 2009; however, unfortunately its increase has not improved as much as other cancers over the same period [3]. This is because clinicians face considerable challenges in visually identifying oral neoplasia at an early stage, leading to many diagnoses occurring late in neoplasia progression [3,4].

Currently disease progression, surgical margins, metastasis and extent of invasion are decided based on diagnostic methods such as X-rays, CT scans or PET images carried out prior to surgery [5,6]. These techniques, though clinically useful, have safety concerns, cannot predictably detect tumors less than 1 cm in diameter (equating to greater than 1 million cancerous cells), and cannot be generated in real time to guide the surgeon intra-operatively.

Address all correspondence to: Deepak Kademani, DMD MD FACS, University of Minnesota, Department of Oral and Maxillofacial Surgery, Moos Tower 7-174G, 515 Delaware Street, Minneapolis, MN, 55455, USA. E-mail: kadem001@umn.edu
Received 16 December 2013; Revised 16 December 2013; Accepted 20 December 2013

http://dx.doi.org/10.1016/j.tranon.2014.02.006

In recent years, there have been a number of scientific approaches to the problem of oral lesion detection (i.e. ViziLite, VELscope, Trimira, OralCDx, etc.). However, the effectiveness of these technologies is inconsistent [5,7]. The literature suggests that these modalities fail to noticeably improve the detection of oral carcinomas from standard head and neck examinations routinely performed by physicians [7]. A major reason for the inconsistency, poor specificity and inability to detect earlier stage cancer is the oversight of these technologies to target advanced stage anatomical changes instead of early stage molecular level alterations.

Optical molecular imaging provides a non-invasive, *in vivo*, rapid and cost effective method to detect early molecular level changes in neoplastic tissue, based on its ability to specifically analyze molecules of interest. More importantly, optical molecular imaging can be performed with minimum training, increasing its potential to be used in the general physicians' office. Possible targets for optical imaging are the glycoproteins and glycolipids on the cell surface. These cellular glycomolecules are completed during the post-translational event called glycosylation, which is known to be abnormal in human disease progression such as carcinogenesis and metastasis [8–10]. This irregular glycosylation results in varying glycosyl residues on the cell surface during pathological changes, highlighting the clinical importance of this alteration as a potential target by which to detect oral cancer.

A prime example of aberrant glycosylation in carcinogenesis is the overexpression of sialyl Lewis A and sialyl Tn antigen in cancers of the pancreas, colon, stomach and esophagus [11,12]. Moreover, increased sialytransferases and sialic acid content on cell glycoconjugates has long been linked to oral cancer and malignant transformation [13,14]. Increased sialic acid content can reach up to 10e+09 sialic acid residues per tumor cell [15]. Further, Rajpura et al. showed statistically significantly higher levels of sialic acid in oral cancer patients compared to normal patients (63.70mg/dl versus 30.25mg/dl, respectively; $P < .001$, 41 patients) [16]. Silvia et al. and Joshi et al. showed similar significant results for sialic acid overexpression in oral cancer patients [17,18].

Specific glycan changes can be targeted using lectins. Lectins are proteins or glycoproteins of non-immune origin that bind non-covalently to specific oligosaccharide chains extending extracellularly from glycoproteins or glycolipids [19]. Lectins exhibit high specificity in recognizing their specific sugar moieties, and thus are useful analytical tools to study the alterations in cell surface carbohydrates in diseased stages [15,19–21]. The other advantages of using lectin probes are the ease of production due to their abundance, inexpensiveness, ease of labeling with fluorescent probes, heat stability, stability at low pH, and low toxicities as many are part of the normal human diet [22].

As sialic acid residues are overexpressed during carcinogenesis, an appropriate lectin probe specific to sialic acid could provide an advantageous biomarker for oral cancer detection. One particular lectin of interest is the legume wheat germ agglutinin (WGA), which is a carbohydrate-binding lectin of approximately 36 kDa that selectively recognizes sialic acid and N-acetylglucosaminyl sugar residues [11,14,22]. Furthermore, conjugation of this lectin with a fluorophore could provide an effective non-invasive *in vivo* screening method to visualize premalignant and malignant oral lesions in real time.

The objective of our study was to establish a preclinical screening technique that targets an intrinsic fluorophore, nicotinamide adenine dinucleotide (NAD^+/NADH), and sialic acid expression, using fluorescent conjugated WGA, to screen for oral cancers. This proof-of-concept preclinical study will be used to guide later clinical evaluation studies.

Materials & Methods

Clinical Sample Set

Freshly extracted tissue samples were obtained either from patients diagnosed with oral cancer or from scalpel biopsies acquired from patients suspected of having oral cancer. In addition, punch biopsies were acquired from patients suspected to have oral cancer, which entered the study *via* the walk-in clinic. All seven patients gave their written informed consent to participate, and the study was reviewed and approved by the Institutional Review Boards at the University of Minnesota and the Mazumdar Shaw Cancer Center in Bangalore, India. Paired biopsies of clinically normal and abnormal oral mucosa were acquired with patient morbidity in mind, and did not deviate from normal clinical practice (Figure 1). Normal tissue biopsies either came from tissue adjacent to the surgical margin or from a slight extension of suspicious lesion margin (Figure 1). Upon extraction, tissue samples were placed in 1× phosphate buffered saline (PBS) (Sigma Aldrich, Milwaukee, WI) to prevent dehydration and then were immediately used for testing. All materials were used as received, unless noted otherwise.

Topical Application of Lectin Probe

To initially demonstrate the efficacy of fluorescently labeled lectins, Alexa Fluor 647 conjugated WGA (AF647-WGA) (Invitrogen, Carlsbad, CA) was used to target sialic acid residues on the cells' surfaces. This specific fluorophore was used since tissue autofluorescence is minimal in the far red and near-infrared spectrums [23]. Specifically, AF647-WGA (5μM titration in 1×PBS, pH 7.4) was topically applied to the tissue samples in the presence of 10 v/v% dimethylsulfoxide (DMSO) (Sigma Aldrich, Milwaukee, WI). DMSO was used as a permeation enhancer to improve delivery of the lectin conjugate through the epithelium of the tissue samples.

Alexa Fluor 350 conjugated WGA (AF350-WGA) (Invitrogen, Carlsbad, CA) (20μM titration in 1×PBS, pH 7.4, and 10 v/v% DMSO) was then used to demonstrate that analogous results could be obtained in the UV spectrum. The molar concentration of AF350-WGA was increased compared to AF647-WGA to overcome possible autofluorescence background signals. Furthermore, the use of a UV fluorophore allowed for the direct comparison of tissue autofluorescence to the fluorescence of AF350-WGA binding. Briefly, tissue autofluorescence in the UV spectrum at 365nm is largely due to an endogenous fluorophore called nicotinamide adenine dinucleotide (NAD^+/NADH) [24,25]. This physiologically important coenzyme is interesting in the fact that its reduced form (NADH) is fluorescent at 365nm whereas its oxidized form (NAD^+) is not. Due to changes in metabolism during oral carcinogenesis, oral cancer cells have lower levels of NADH [24,25]. To establish an autofluorescence background value at 365nm, epi-illumination (reflectance) images were acquired from the tissue samples under narrow band illumination of UV light using a 365nm ± 7.25nm LED (Opto Technology Inc., Wheeling, IL).

Both Alexa Fluor conjugated WGA molecules were subjected to the following protocols which were slightly modified according to the tissue type of the patients. Pilot experiments were conducted to

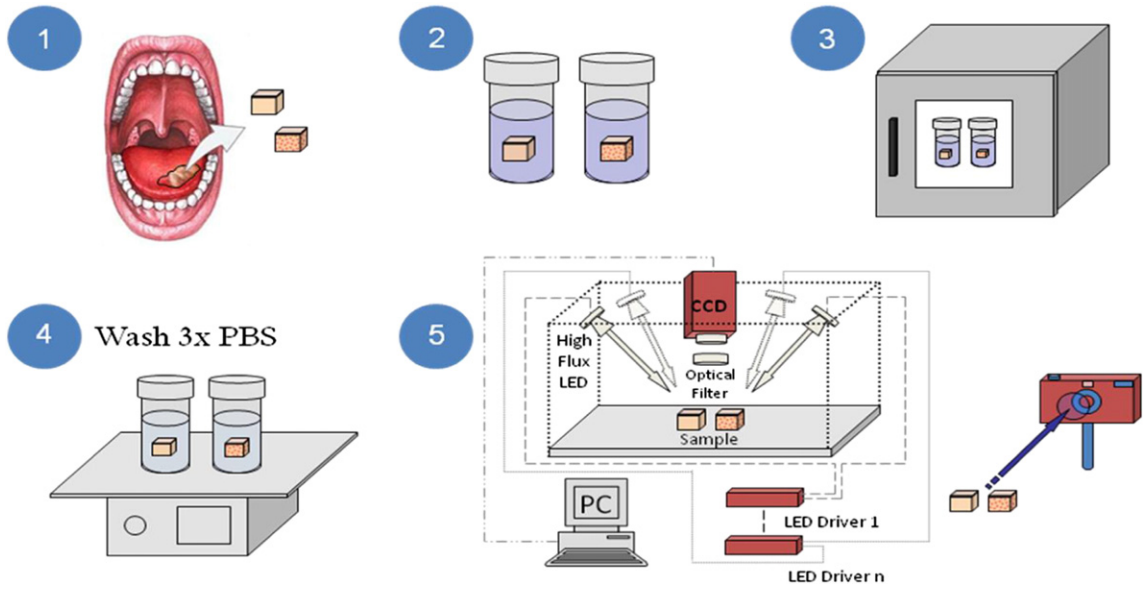

Figure 1. Schematic representation of tissue processing and imaging. The figure represents the surgical resection of abnormal and control tissue (1), pre-incubated in PBS (2) and in WGA-fluorophore for an hour (3). The samples are subsequently washed in PBS 3 times (4) and then imaged using a custom designed optical imaging system capable of multispectral epi-illumination (reflectance) imaging (5).

ensure that the following protocols only allowed for superficial tissue staining (data not shown).

For biopsies. The tissue samples were stained with 0.5 ml to 2ml of WGA fluorescent probe and incubated for one hour at 37°C. The tissue samples were then washed three times in succession, the first time with 30 ml 1x PBS in 10 v/v% DMSO, and the second and third times with 30 ml 1x PBS.

For complete resection samples. The tissue was stained with 4 ml of WGA fluorescent probe and incubated for one hour at 37°C. The tissue was then washed three times in succession, the first time with 100 ml 1x PBS in 10 v/v% DMSO, and the second and third times with 100 ml 1x PBS. The larger volume used for resected tissue was necessary as these tissue samples were physically larger than the biopsies.

Lastly, the molecular specificity of the WGA binding was assessed by pre-incubating the AF350-WGA with its inhibitory sugar N-acetyl glucosamine at a concentration of 0.5M. This was performed for 30 min at 37°C. The uninhibited and inhibited conjugated AF350-WGA were then applied to different cancerous biopsy samples taken from the same surgical site and incubated for one hour at 37°C. A cancerous biopsy that was not incubated with any WGA was also used as a control for comparison purposes. The normal tissue sample only received uninhibited AF350-WGA, and was incubated simultaneously with the cancerous biopsies. Tissue samples were then washed as stated previously for biopsies and imaged as described in the next section. This inhibition procedure was derived from similar lectin inhibition procedures established in the literature [8,26–28].

Optical System

Following incubation in the WGA-fluorophore DMSO mixture and washing, tissue surface sialic acid expression in normal and neoplastic oral tissues was measured using high-resolution fluorescence imaging. Reflectance and fluorescence images were acquired using a custom designed optical system. The imaging system (Figure 1) allowed for epi-illumination data acquisition to be obtained at multiple wavelengths, specifically white light illumination, UV (365nm ± 7.25nm) and red (630nm ± 10nm). Excitation illumination was performed with high intensity light emitting diodes (LEDs) (Opto Technology Inc., Wheeling, IL) collimated and directed to evenly illuminate the entire field of view (10 cm × 10 cm). Conversely, due to space constraints, the white fluorescent light was mounted at the rear of the optical system. The high intensity LEDs were powered using constant current LED drivers (LuxDrive a division of LEDdynamics Inc, Randolph, VT), so that invariable radiant power could be achieved. Paired sets of biopsies were imaged together to ensure they received identical imaging conditions (*i.e.* detector gain and radiant illumination power). Photons generated within the tissue samples were then detected by a scientific CCD camera (Coolsnap HQ, Photometrics, Tucson, AZ) using the appropriate bandpass and longpass filters (Thorlabs, Newton, NJ). The filters for each combination have been summarized in Table 1. Lastly, a Canon PowerShot A3100 IS digital camera (Canon U.S.A. Inc., Melville, NY) was mounted within the optical system to capture fluorescent images that would more accurately demonstrate the conditions observed within the clinical setting without filtering. Fluorescence overlay images were created by superimposing the fluorescence images over the white light images; this was performed for registration and clinical relevance.

Quantification of Imaging Data

Wide-field fluorescence images of the oral tissue samples obtained before and after incubation were quantitatively analyzed using ImageJ (NIH, Bethesda, MA) to calculate the mean fluorescence intensity

Table 1. Excitation and emission filters used in this study.

	365nm High Flux LED	630nm High Flux LED
Excitation	360nm ± 5nm bandpass	640nm ± 5nm bandpass
Fluorescence	400nm longpass and 450nm ± 20nm bandpass	650nm longpass and 680nm ± 5nm bandpass

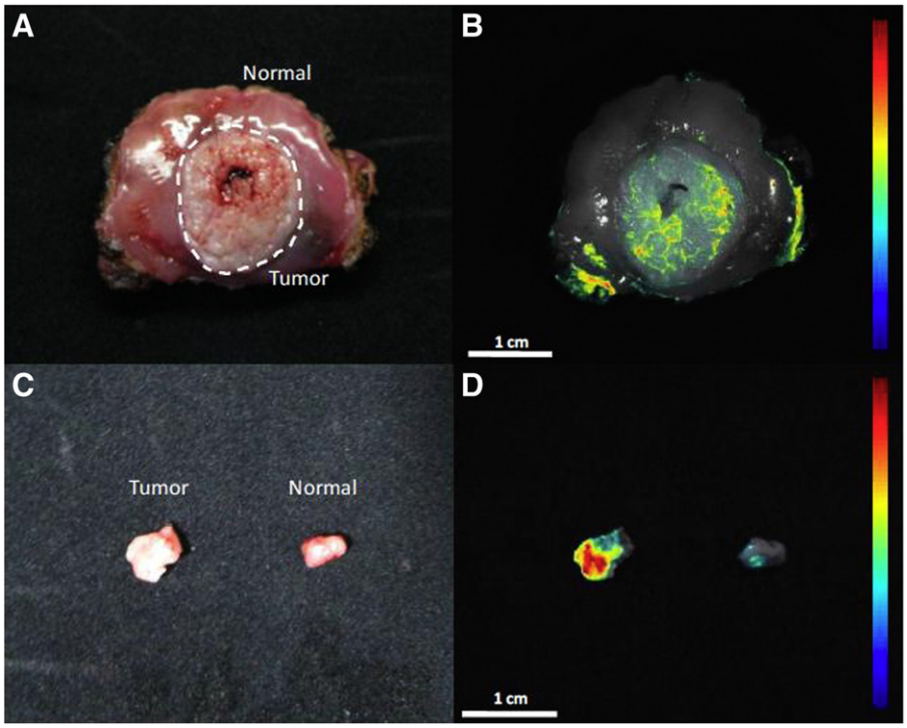

Figure 2. Representative white light and fluorescence overlay images of complete resections and biopsies from the same patient. The freshly resected specimen (A & B) and biopsies (C & D) were imaged under white light (A & C) and fluorescence (B & D). The whole specimen was labeled with AF647-WGA (B), while the biopsies were labeled with AF350-WGA (D). Both fluorophore conjugated WGA lectins resulted in enhanced fluorescence in cancerous tissue compared to normal tissue. The fluorescence seen on the periphery of the normal tissue specimen (B) is due to AF647-WGA staining of the stroma layer, which was exposed following resection. The color coded intensity scale and the magnifications are indicated in the figure.

(MFI) of a region-of-interest on the tissue's epithelial surface. ImageJ was also used to obtain a measure of the camera background noise, and the measured MFI's were recorded with the static background noise subtracted. To quantify a measure of WGA binding affinity between normal and cancerous tissue, the signal-to-noise ratio (SNR) between those samples was determined by taking the MFI value from the diseased tissue and dividing it by the MFI value from the normal tissue; it should be noted that the same region-of-interest was used to calculate MFI values for the normal and cancerous tissue. The SNR for autofluorescence is the inverse of this definition as tumor autofluorescence is lower than normal tissue autofluorescence due to lower NADH levels [24,25]; thus this SNR is the MFI of the normal tissue divided by the MFI of the cancerous tissue. This SNR calculation provides the most robust measure of differential fluorescent values, since the samples were imaged together and no other manipulation of the raw values were made.

Pathological Diagnosis

Following imaging, each sample received a unique label to remove any trace of patient information so that the pathological diagnosis was

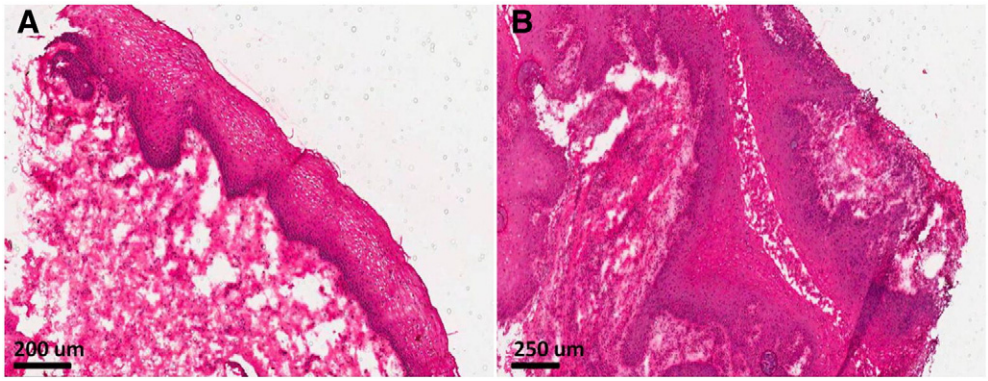

Figure 3. Histology images of tissue in Fig 2. Biopsy specimens shown in Fig 2 were confirmed normal and cancerous via a standard H&E stain. Fig 3A shows the normal tissue epithelium whereas Fig 3B shows stage I squamous cell carcinoma, which is characteristic of numerous large, dense and atypical nuclei with irregular patterning. Similar histology results were obtained for all other patients.

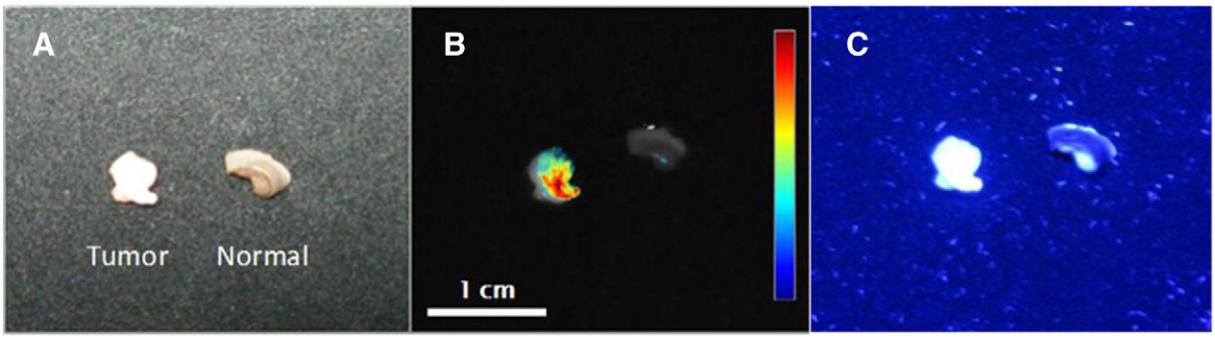

Figure 4. Representative images of whole biopsies. Biopsy specimens (tumor and normal) derived from patients were labeled with AF350-WGA and then imaged under white light (A) and fluorescence (B & C) in two different patients. Fig 4B is an overlay image taken with the scientific camera whereas Fig 4C is an image taken with the digital camera. Again, localization of the lectin on the cancerous tissue is seen. AF350-WGA results in fluorophore emission that is easily seen with the naked eye (C). The color coded intensity scale and the magnifications are indicated in the figure.

blinded and separated from the fluorescent staining results. Tissue samples were then bisected so that a portion was fixed in formaldehyde and paraffin embedded, and another could be used for frozen section analysis for quick histological diagnosis. True pathological diagnosis consisted of a routine hematoxylin and eosin (H&E) stain performed and analyzed by a board certified pathologist. The pathological diagnosis was then classified into the following three categories: (1) normal, (2) dysplasia and (3) cancer with stage. All specimens were then returned to the Pathology Department of the Narayana Hrudayalaya Multispecialty Hospital and Mazumdar-Shaw Cancer Center.

Statistical Analysis

Data are presented as mean ± SD. Statistical analysis of *ex vivo* fluorescence measurements was conducted using a 2-tailed, paired Student's t test. All statistical analyses were performed using a 95% confidence interval, which relates to a P value < .05 being statistically significant.

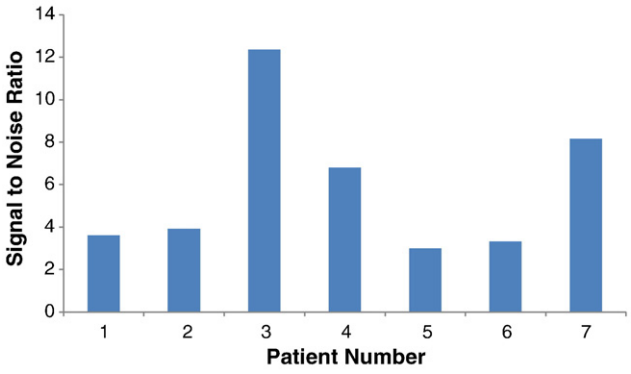

Figure 5. Distinction between the normal and tumor samples in terms of signal to noise ratios (SNR) using AF350-WGA. The cancerous tissue displayed statistically significantly higher fluorescence than the normal tissue with an average SNR of 5.88 ± 3.46 (P = .00046).

Results

Fluorescence Imaging Using WGA Lectin Fluorophore Conjugates

Both AF647 and AF350 conjugated WGA yielded similar binding results. This can be seen in Figure 2 which shows white light (Figure 2*A* and *C*), red light (Figure 2*B*), and UV (Figure 2*D*) excitation images of cancerous and normal tissues from the same patient stained with both fluorophore conjugates. The excised tissue was stained with AF647-WGA while the smaller tissue biopsies, from the same excised tissue specimen, were stained with AF350-WGA. The fluorescence seen on the periphery of the normal tissue specimen (B) is due to AF647-WGA staining of the stroma layer, instead of the epithelial layer; the stroma layer was exposed due to tissue resection. However, the clinical topical application of WGA will not concern the deeper tissue layers and will only analyze epithelial glycan expression profiles. Therefore, these recorded intensity measurements were omitted from ROIs of epithelial fluorescence. Histological evaluation of the tissue samples revealed normal epithelium (Figure 3*A*) and stage I squamous cell carcinoma (Figure 3*B*) for the normal and cancerous tissue samples, respectively. This shows it is

Table 2. Summary of the data collected during experimentation.

PT	Patient #	AF350-WGA Fluorescence (FWHM 40)			UV Autofluorescence (FWHM 40)		
		T	N	SNR	T	N	SNR
22	1	1315.19	364.31	3.61	587.12	658.02	1.12
23	2	1255.65	320.82	3.91	217.18	407.83	1.88
25	3	2354.96	190.61	12.36	207.45	181.50	0.87
27	4	2341.97	344.11	6.81	804.92	1552.26	1.93
28	5	1377.93	458.09	3.01	459.84	577.40	1.26
29	6	3072.64	923.95	3.33	730.93	784.69	1.07
30	7	2164.93	265.50	8.15	568.341	743.62	1.31
	AVE	-	-	5.88	-	-	1.35
	SD	-	-	3.46	-	-	0.41

The WGA probe yielded statistically significantly greater fluorescence in cancerous tissue compared to normal tissue (SNR of 5.88 ± 3.46, P = .00046). The UV autofluorescence was not statistically significantly different than normal tissue (SNR of 1.35 ± 0.41, P = .098). The SNR of the AF350-WGA probe was statistically significantly larger than the SNR for UV autofluorescence (P = .0049).

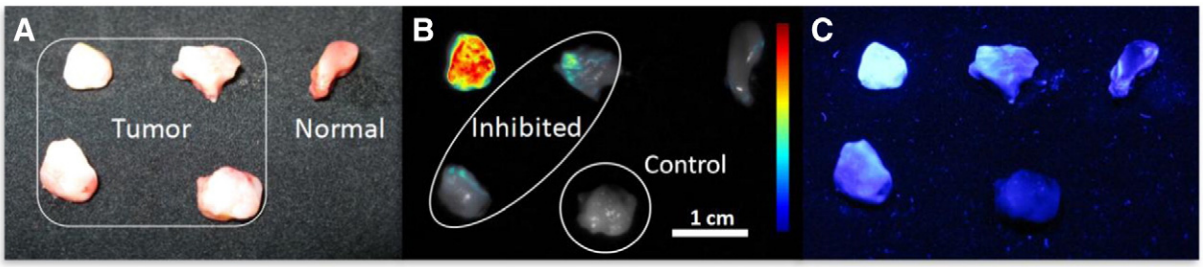

Figure 6. Molecular binding specificity experiment with the inhibitory sugar N-acetyl glucosamine. Biopsy specimens, tumor and normal, were derived from the resection specimen of a single patient and incubated with inhibited (within the oval) and uninhibited AF350-WGA conjugate. A sample of the tumor was not incubated with any WGA and kept as a control. The specimens were imaged under white light (A) and fluorescence (B & C). Fig 6B is an overlay image taken with the scientific camera whereas Fig 6C is an image taken with the digital camera. Pre-incubation of AF350-WGA with the inhibitory sugar resulted in a 3 fold decrease in fluorescence of the cancerous tissue; however, this fluorescence was still greater than fluorescence from normal tissue incubated with uninhibited AF350-WGA. No incubation with WGA resulted in very little fluorescence for the cancerous control sample. These results demonstrate that the lectin binding is indeed molecularly specific to sialic acid residues that are overexpressed on cancerous tissue. The tumor and normal specimens, intensity scale and magnification are indicated in the figure.

possible to specifically target abnormal glycan expression on cancerous tissue utilizing different fluorophores conjugated to WGA.

Figure 4*A* shows a different set of biopsy samples visualized under white light following treatment with the AF350-WGA probe. The fluorescent lamp used for white light imaging may have caused uneven tissue illumination, resulting in the cancerous tissue looking brighter in Figure 4*A*. However, tissue appearance differences between normal and diseased tissue is well established due to increased cell density, protein amounts, etc. Typically, these lesions are often times whiter in appearance which would have caused them to appear brighter under white light imaging. Nevertheless, increased probe fluorescence is noted on the tumor specimen and not the normal specimen (Figure 4*B*), proving the specificity of the probe for the overexpressed glycan residues on the tumor surface. Lastly, Figure 4*C* shows a digital camera image of tissue biopsies incubated in AF350-WGA to capture fluorescent images that would more accurately demonstrate the conditions observed within a clinical setting; this image shows the enhanced fluorescence is easily visible with the naked eye.

Similar results were seen for all tissue samples tested with AF350-WGA and are summarized in Figure 5 and in Table 2. Figure 5 shows the patient/tissue samples' SNR for AF350-WGA testing. The AF350-WGA fluorescence of the cancerous tissue was statistically significantly higher than that of normal tissue with an average SNR of 5.88 ± 3.46 (P = .00046, Table 2). The differences observed amongst the SNRs can be attributed to the fact that sialic acid overexpression is dependent on patient variability, disease progression, cancer aggressiveness, etc. However, it is important to note that all patients displayed SNRs greater than 3. The UV autofluorescence of the cancerous tissue displayed an average SNR of 1.35 ± 0.41 and was not statistically significantly different than normal tissue (P = .098, Table 2). The SNR of AF350-WGA was statistically significantly larger than the SNR for UV autofluorescence (P = .0049, Table 2) with it being at least double the ratio in all seven patients.

Inhibitory Sugar Experiments Indicate the Specificity of the Assay

To further validate the specificity of the WGA binding conjugate, inhibitory experiments were carried out with N-acetyl glucosamine which serves to block the available binding sites of WGA prior to sample application. Pre-incubation of AF350-WGA with the sugar resulted in a threefold decrease in fluorescence intensities of the cancerous tissue (Figure 6), indicating that the soluble sugar competitively inhibited the WGA from binding to the overexpressed glycan residues on the cancerous cell surface. Interestingly, the inhibited AF350-WGA still resulted in higher fluorescence intensity values from the cancerous tissue when compared to the normal tissue (Figure 6*B* and *C*). This clearly demonstrates that neoplastic tissue exhibits a much higher content of overexpressed cell surface glycans compared to normal tissue, further supporting WGA's specificity for the overexpressed sialic acid on the cancerous cell surface. Lastly, the cancerous and normal biopsies incubated with either uninhibited or inhibited AF350-WGA resulted in greater fluorescence than the control tumor sample that was not incubated with any AF350-WGA. This demonstrates that the observed fluorescence from tissue stained with the lectin conjugate is not a result of intrinsic tissue autofluorescence at the excitation wavelength of 365nm.

Pathological Diagnosis

Histological analysis revealed that 4/7 patients had stage I cancer, 1/7 had stage II cancer, and 2/7 had stage IV cancer. Of the seven patients, 6/7 exhibited squamous cell carcinoma while 1/7 exhibited dysplasia. All normal biopsies were confirmed to be free from disease. The histological results are summarized in Table 3. Histology pictures for the tissue in Figure 2 can be seen in Figure 3. Here normal tissue

Table 3. Summary of paired biopsy sets listing anatomical site in the oral cavity and the pathological diagnosis.

Patient Number	Sex	Age	Anatomical Site	Stage	Pathological Diagnosis
1	M	50	BM	I	SCC/Normal
2	F	55	BM	IV	SCC/Normal
3	M	55	BM	II	SCC/Normal
4	M	70	FOM	I	SCC/Normal
5	F	56	BM	I	Dysplasia/Normal
6	M	61	BM	I	SCC/Normal
7	F	47	BM	IV	SCC/Normal

BM: Buccal Mucosa; FOM: Floor of Mouth; SCC: Squamous Cell Carcinoma.

was histologically verified (Figure 3*A*), whereas cancerous tissue was verified as stage I squamous cell carcinoma (Figure 3B).

It should be noted that the effect of AF350 and AF647 lectin binding on H&E staining was tested by comparing lectin labeled slices with unlabeled control slices from the same biopsy set. Comparison of these slices showed no effect of lectin labeling on H&E staining (data not shown). Furthermore, H&E staining was identical for normal and clinically abnormal tissue independent of the degree of staining with Alexa Fluor lectin conjugates.

Discussion

The use of molecular and biochemical changes as a basis to develop early detection methods of oral cancer were explored in this manuscript. The lectin WGA was primarily chosen for this application as it has high affinity for sialic acid and N-acetyl glucosamine residues which are known to be overexpressed in neoplastic tissue due to aberrant glycosylation [13,14,29–31]. Furthermore, the relative expression of these sialic acid residues in the epithelium is suggested to be representative of tumor prognosis [16,18,32]. The data presented here demonstrate that WGA fluorophore probes can agglomerate on cancer cells overexpressing these glycomolecules, successfully yielding statistically higher fluorescence in cancerous tissue than normal tissue. Additionally, the WGA fluorophore probes resulted in a higher SNR than tissue UV autofluorescence at 365nm. Furthermore, through inhibitory binding studies with WGA it was shown that the lectin binding is molecularly specific to these glycans since inhibited WGA resulted in decreased tissue fluorescence, highlighting that the WGA is in fact binding to cellular glycans overexpressed in cancerous tissues. Lastly, this experiment showed that fluorescence intensity differences are not due to tissue diffusion variations between normal and tumor tissues (i.e. leaking vasculature or compromised mucosa). Our data demonstrate that the use of WGA fluorophore probes is a significant improvement over current autofluorescent methods. This procedure provides reproducible SNRs for reliably differentiating normal tissue from cancerous tissue in the oral mucosa that can be viewed unaided by the naked eye.

Both exogenous fluorophores (AF647 and AF350) tested showed similar results even though the fluorophores are on the opposite ends of the visible spectrum. The AF647-WGA probe was used to initially test the feasibility of cancer detection as there is negligible tissue autofluorescence in the far-red and near-infrared spectrums [23], providing a measure of confidence that the fluorescence obtained was from the binding of the lectin to glycoconjugates. Additionally, near infrared wavelengths can penetrate further into the tissue [33]. However, since we are imaging the probe on the superficial tissue surface, light propagation into the tissue is not a concern and did not seem to enhance the SNRs in this experiment. The disadvantage of utilizing near-infrared fluorophores is the fact that a camera and narrow bandpass filtering is needed since visualization is outside of the visible spectrum, and near-infrared fluorophores exhibit small stokes shifts. Previous work of ours detailed the use of AF647-WGA for oral cancer detection; however, the data is not shown in this manuscript (besides the single patient comparison of AF350-WGA and AF647-WGA) since this paper focused on developing a clinically useful tool without the need for complex filters and cameras. As such, most of the presented data was with AF350-WGA, which allowed for fluorophore emission easily visible to the naked eye. Furthermore, as the AF350 is in the UV spectrum, there is more energy per photon which yields a larger stokes shift for UV fluorophores; a larger stokes shift is advantageous to allow for easier discrimination of excited and emitted light. Combined, these features make the AF350-WGA more suitable for clinical use as additional equipment is not required.

Previously, researchers have examined intrinsic fluorescent molecules and tissue reflectance properties to differentiate between normal and cancerous tissue. For example, commercially available devices (VELscope, ViziLite, etc.) have been developed to analyze tissue autofluorescence for cancerous tissue. However, these devices were identified as ineffective adjuncts to current white light head and neck exams as well as histological methods as they lack adequate specificity and sensitivity to accurately diagnose oral cancer [34,35]. Similar conclusions were seen in our data which showed suggestive differences in autofluorescence between normal and cancerous tissue at 365nm ($P = .098$). Another group demonstrated that fluorescently labeled glucose preferentially localized in cancerous tissue due to increased metabolic activity. This approach was favorable and lead to a SNR of 3.7 [36]; however, this is lower than the SNR reported in this manuscript (5.88). In a recent study by Bird-Leiberman, they showed that alteration of cell surface glycans in Barret's esophagus from dysplasia to adenocarcinoma can be effectively visualized using a fluorophore bound to WGA [22]. The WGA binding to the altered cell surface glycans was highly specific and aided in the discovery of lesions that would have been missed during conventional endoscopy [22]. The results presented by Bird-Leiberman et al. are very similar to the data shown in this study, which confirms the use of lectin molecules as potential markers of neoplasia in lesions that cannot be visualized clinically in white light. Moreover, this approach can be used to determine surgical boundaries in the oral cavity prior to tumor resection.

One of the limitations of the study has been the usage of the permeation chemical DMSO. Although FDA approved for some applications, it does have some minor side effects including skin rash, nausea, and headache [37,38]. Another limitation is that tissue samples were incubated with the WGA-fluorophore solution for 1 hour which would not be clinically feasible. These and other limitations will be addressed through additional studies to determine the most adequate composition of AF350-WGA solution for clinically relevant cancer detection.

This study investigated the efficacy of fluorescence imaging using topically applied lectin-fluorophore conjugates as compared to conventional tissue autofluorescence in distinguishing tumor tissue. The results revealed that the changes in glycosylation could differentiate normal from cancerous tissues in the oral cavity with high SNRs. Therefore, this technique seems promising as a non-invasive screening method for premalignant and malignant mucosal tumors, and as a method for defining surgical margins and monitoring cellular changes over time. Provided technologies that target cancer on a molecular level, clinicians could effectively recognize lesions in earlier stages, thereby enabling early detection and treatment. To further evaluate this approach for oral cancer screening, *in vivo* testing with a larger sample size needs to be performed to obtain sensitivity and specificity values. Nevertheless, to the best of our knowledge, the authors have, for the first time, demonstrated that topical application of lectin probes to mucosal epithelial tissues followed by molecular imaging of the tissues can be used to spatially differentiate cancerous and normal tissue of the oral cavity.

References

[1] Curtis RE (2006). New malignancies among cancer survivors : SEER cancer registries, 1973-2000, Vol. U.S. Dept. of Health and Human Services. Washington, DC: National Institutes of Health, National Cancer Institute; 2006.

[2] Ries LAG (2007). Cancer survival among adults : U.S. SEER program, 1988-2001, patient and tumor characteristics, Vol. U.S. Bethesda, MD: Department of Health and Human Services, National Institutes of Health, National Cancer Institute; 2007.

[3] SEER Program (National Cancer Institute (U.S.))National Center for Health Statistics (U.S.)National Cancer Institute (U.S.)Program Surveillance, National Cancer Institute (U.S.)Statistics Branch Cancer, National Cancer Institute (U.S.) Control Research Program Cancer (1993). SEER cancer statistics review. U.S. Dept. of Health and Human Services, Public Health Service, National Institutes of Health, National Cancer Institute: City; 1993. p. v.

[4] Emerick KS, Leavitt ER, Michaelson JS, Diephuis B, Clark JR, and Deschler DG (2013). Initial clinical findings of a mathematical model to predict survival of head and neck cancer. *Otolaryngol Head Neck Surg* **149**, 572–578.

[5] Awan KH, Morgan PR, Warnakulasuriya S. Evaluation of an autofluorescence based imaging system (VELscope) in the detection of oral potentially malignant disorders and benign keratoses. Oral Oncology 47, 274–277.

[6] Drezek R, Sokolov K, Utzinger U, Boiko I, Malpica A, Follen M, and Richards-Kortum R (2001). Understanding the contributions of NADH and collagen to cervical tissue fluorescence spectra: modeling, measurements, and implications. *J Biomed Opt* **6**, 385–396.

[7] Huber MA (2012). Adjunctive diagnostic aids in oral cancer screening: an update. *Tex Dent J* **129**, 471–480.

[8] Vigneswaran N, Peters KP, Hornstein OP, and Diepgen TL (1990). Alteration of cell surface carbohydrates associated with ordered and disordered proliferation of oral epithelia: a lectin histochemical study in oral leukoplakias, papillomas and carcinomas. *Cell Tissue Kinet* **23**, 41–55.

[9] Sakamoto I, Tezuka K, Fukae K, Ishii K, Taduru K, Maeda M, Ouchi M, Yoshida K, Nambu Y, and Igarashi J, et al (2012). Chemical synthesis of homogeneous human glycosyl-interferon-beta that exhibits potent antitumor activity in vivo. *J Am Chem Soc* **134**, 5428–5431.

[10] He J, Liu Y, Zhu TS, Xie X, Costello MA, Talsma CE, Flack CG, Crowley JG, Dimeco F, and Vescovi AL, et al (2011). Glycoproteomic analysis of glioblastoma stem cell differentiation. *J Proteome Res* **10**, 330–338.

[11] Bychkov V and Toto PD (1986). Wheat germ and peanut agglutinin binding to normal, dysplastic and neoplastic cervical epithelium. *Gynecol Obstet Invest* **21**, 158–163.

[12] Bychkov V and Toto PD (1986). Lectin binding to normal human endometrium. *Gynecol Obstet Invest* **22**, 29–33.

[13] Sanjay P, Hallikeri K, and Shivashankara A (2008). Evaluation of salivary sialic acid, total protein, and total sugar in oral cancer: a preliminary report. *Indian J Dent Res* **19**, 288.

[14] May D and Sloan P (1991). Lectin binding to normal mucosa, leukoplakia and squamous cell carcinoma of the oral cavity. *Med Lab Sci* **48**, 6–18.

[15] Kleinert R and Radner H (1987). *Lectin binding in meningiomas Neuropathology and applied neurobiology* **13**, 263–272.

[16] Rajpura KB, Patel PS, Chawda JG, and Shah RM (2005). Clinical significance of total and lipid bound sialic acid levels in oral pre-cancerous conditions and oral cancer. *J Oral Pathol Med* **34**, 263–267.

[17] Silvia CWD, Vasudevan D, and Prabhu KS (2001). Evaluation of serum glycoproteins in oral carcinoma. *Indian J Clin Biochem* **16**, 113–115.

[18] Joshi M and Patil R (2010). Estimation and comparative study of serum total sialic acid levels as tumor markers in oral cancer and precancer. *J Cancer Res Ther* **6**, 263.

[19] Karuna V, Shanthi P, and Madhavan M (1992). Lectin binding patterns in benign and malignant lesions of the breast. *Indian journal of pathology & microbiology* **35**, 289.

[20] Narita T and Numao H (1992). Lectin binding patterns in normal, metaplastic, and neoplastic gastric mucosa. *J Histochem Cytochem* **40**, 681–687.

[21] Ohuchi N, Nose M, Abe R, and Kyogoku M (1984). Lectin-binding patterns of breast carcinoma: significance on structural atypism. *Tohoku J Exp Med* **143**, 491–499.

[22] Bird-Lieberman EL, Neves AA, Lao-Sirieix P, O'Donovan M, Novelli M, Lovat LB, Eng WS, Mahal LK, Brindle KM, and Fitzgerald RC (2012). Molecular imaging using fluorescent lectins permits rapid endoscopic identification of dysplasia in Barrett's esophagus. *Nat Med* **18**, 315–321.

[23] Bremer C, Tung C-H, Bogdanov A, and Weissleder R (2002). Imaging of Differential Protease Expression in Breast Cancers for Detection of Aggressive Tumor Phenotypes1. *Radiology* **222**, 814–818.

[24] Majumder S, Gupta P, and Uppal A (1999). Autofluorescence spectroscopy of tissues from human oral cavity for discriminating malignant from normal. *Lasers Life Sci* **8**, 211–227.

[25] Majumder S, Mohanty S, Ghosh N, Gupta P, Jain D, and Khan F (2000). A pilot study on the use of autofluorescence spectroscopy for diagnosis of the cancer of human oral cavity. *Current Sci* **79**, 1089–1094.

[26] Saku T and Okabe H (1989). Differential lectin-bindings in normal and precancerous epithelium and squamous cell carcinoma of the oral mucosa. *J Oral Pathol Med* **18**, 438–445.

[27] Bhavanandan VP and Katlic AW (1979). The interaction of wheat germ agglutinin with sialoglycoproteins. The role of sialic acid. *J Biol Chem* **254**, 4000–4008.

[28] Geoghegan WD and Ackerman GA (1977). Adsorption of horseradish peroxidase, ovomucoid and anti-immunoglobulin to colloidal gold for the indirect detection of concanavalin A, wheat germ agglutinin and goat anti-human immunoglobulin G on cell surfaces at the electron microscopic level: a new method, theory and application. *J Histochem Cytochem* **25**, 1187–1200.

[29] Saitoh O, Wang W, Lotan R, and Fukuda M (1992). Differential glycosylation and cell surface expression of lysosomal membrane glycoproteins in sublines of a human colon cancer exhibiting distinct metastatic potentials. *J Biol Chem* **267**, 5700–5711.

[30] Aubert M, Panicot L, Crotte C, Gibier P, Lombardo D, Sadoulet M-O, and Mas E (2000). Restoration of α (1, 2) fucosyltransferase activity decreases adhesive and metastatic properties of human pancreatic cancer cells. *Cancer Res* **60**, 1449–1456.

[31] Raval G, Patel D, Parekh L, Patel J, Shah M, and Patel P (2003). Evaluation of serum sialic acid, sialyltransferase and sialoproteins in oral cavity cancer. *Oral Dis* **9**, 119–128.

[32] Dabelsteen E, Clausen H, and Mandel U (1992). Carbohydrate changes in squamous cell carcinomas. *APMIS Suppl* **27**, 130.

[33] Ntziachristos V, Yodh A, Schnall M, and Chance B (2000). Concurrent MRI and diffuse optical tomography of breast after indocyanine green enhancement. *Proc Natl Acad Sci* **97**, 2767–2772.

[34] Rana M, Zapf A, Kuehle M, Gellrich NC, and Eckardt AM (2012). Clinical evaluation of an autofluorescence diagnostic device for oral cancer detection: a prospective randomized diagnostic study. *Eur J Cancer Prev* **21**, 460–466.

[35] Matsumoto K (2011). Detection of potentially malignant and malignant lesions of oral cavity using autofluorescence visualization device. *Kokubyo Gakkai Zasshi* **78**, 73–80.

[36] Nitin N, Carlson AL, Muldoon T, El-Naggar AK, Gillenwater A, and Richards-Kortum R (2009). Molecular imaging of glucose uptake in oral neoplasia following topical application of fluorescently labeled deoxy-glucose. *Int J Cancer* **124**, 2634–2642.

[37] Swanson B (1985). Medical use of dimethyl sulfoxide (DMSO). *Revi Clin Basic Pharmacol* **5**, 1.

[38] Perez-Marrero R, Emerson L, and Feltis J (1988). A controlled study of dimethyl sulfoxide in interstitial cystitis. *J Urol* **140**, 36.